

Gapfilling Interrupted Helioseismic Data with the EM Algorithm*

M. Roth^{1**} and Yu. D. Zhugzhda^{2***}

¹*Kiepenheuer-Institut für Sonnenphysik, Schöneckstr. 6, 79104 Freiburg, Germany;*

Max-Planck-Institut für Sonnensystemforschung, Max-Planck-Str. 2, 37191 Katlenburg-Lindau, Germany

²*Institute of Terrestrial Magnetism, Ionosphere and Radio Wave Propagation, Russian Academy of Sciences, Troitsk, Moscow oblast, 142190 Russia;*

Kiepenheuer-Institut für Sonnenphysik, Schöneckstr. 6, 79104 Freiburg, Germany

Received October 21, 2008

Abstract—Helioseismic data are often interrupted by gaps, which diminish the quality of the data. In the frequency domain, these gaps lead to systematic effects with misleading interpretation of the power spectra. We propose a gap filling method that is based on modeling solar oscillation data with a statistical process, i.e., the stochastic nature of a single oscillation is taken into account by regarding it as realization of an autoregressive (AR) processes of second order. From the whole oscillation time series given as the superposition of the realization of many excited modes, the process parameters are estimated via the expectation maximization (EM) algorithm. Then the estimated model is used to predict the further course of the oscillatory process during occurring gaps. We demonstrate the applicability of this procedure on the basis of both simulations and data obtained with the DIFOS satellite experiment suffering from gaps of 30 min duration occurring regularly every 90 min due to the orbit around the Earth.

DOI: 10.1134/S106377371001007X

Key words: *helioseismology, data recovering, autoregressing.*

1. INTRODUCTION

One central task in helioseismology is to obtain an uninterrupted coverage of solar observations. The reason for this is, that gaps in the data result in side lobes in the Fourier spectra of the solar time series. Hence the estimation of peak locations and therefore the frequency determination of the solar oscillations is affected by systematic effects, e.g., the day-night cycle on Earth results in side-lobes $11.57 \mu\text{Hz}$ around each peak in the power spectra. Moreover the signal-to-noise ratio is reduced, which in total leads to a lower accuracy in the p-mode parameter estimation. With the advent of the networks GONG, BiSON, IRIS, TON, etc., or the space-borne observatories, e.g., SOHO, the occurrence of gaps in the data was greatly reduced, nevertheless a duty cycle of 100% is established in neither of the helioseismic experiments. Especially in helio- and asteroseismic experiments on satellites that orbit the Earth, e.g., DIFOS (Multi-channel Solar Photometer) gaps of ≈ 30 min duration occur every ≈ 90 min. In order to increase the duty cycle in the recorded time series there exists the idea

of filling the gaps by some sophisticated manner. Naturally, it seems to be straight-forward to fill the gaps by a kind of interpolation, e.g., sine-functions. Fossat et al. (1999) compared interpolation methods with a method they called “Repetive Music.” The basic idea of “Repetive Music” is to make use of the autocorrelation of the oscillation signals, which shows secondary maxima of up to 0.7 at a lag of about 4 h (Gabriel 1998). Filling the gap with data collected 4 h prior to the gap results in a high confidence of up to 90%, which is superior to a sine interpolation. Further investigations and improvements of the “Repetive Music” method concentrated on removing the modulation in the power spectrum resulting from the gap-filling method (Fraillon and Appourchaux, 2001).

Another approach was presented by Zhugzhda (1995) who used a non-uniform time transformation for filling gapped time series. The correct choice of the time transformation allows to remove side lobes from the spectrum. However, the efficiency of this method decreases with increasing noise level.

In this contribution we introduce a gap-filling method that is based on modeling oscillation time series by autoregressive processes of second order (AR(2)) and on estimating the process parameters by the Expectation Maximization (EM) algorithm. We

*The article was translated by the authors.

**E-mail: mroth@kis.uni-freiburg.de

***E-mail: yuzef@izmiran.rssi.ru

apply this procedure to simulated time series and time series recorded by the DIFOS experiment aboard the CORONAS-F satellite (Lebedev et al., 2004).

2. MODELING SOLAR OSCILLATIONS BY AN AUTOREGRESSIVE PROCESS

As the solar oscillations are stochastically excited damped harmonic oscillators the measured time series are observations of a stochastic process. The presented gapfilling method is based on modeling the solar oscillation time series by an autoregressive stochastic process. There, the stochastic nature of the modes is taken into account by modeling the measured oscillation amplitude $x(t)$ at an instant t in dependence on its states in the past and some additional noise term $\eta(t)$

$$x(t) = \sum_{i=1}^p a_i x(t-i) + \eta(t), \quad (1)$$

where the parameters a_i are the coefficients of the AR process of order p and $\eta(t) \propto N(0, \sigma^2)$ is a realization of a Gaussian noise process with a zero mean and variance σ^2 , and t is measured in units of the inverse sampling rate. A stochastically excited damped harmonic oscillation is described by an AR process of second order, i.e., $p = 2$ (Honerkamp, 2002)

$$x(t) = a_1 x(t-1) + a_2 x(t-2) + \eta(t). \quad (2)$$

This is the discretized version of the stochastic second order differential equation for the stochastically excited damped harmonic oscillation

$$\ddot{x}(t) = -\gamma \dot{x}(t) + \omega^2 x(t) + \eta(t), \quad (3)$$

where γ is the damping and ω the frequency of the oscillation. The following relations can be established

$$a_1 = 2e^{-1/\tau} \cos(\omega) \quad (4)$$

$$a_2 = -e^{-2/\tau}, \quad (5)$$

where τ is the damping rate of the oscillation due to the friction γ .

An AR process of second order may be interpreted as a multivariate AR process of first order AR(1) by expanding the dimension of the one-dimensional state x to a two-dimensional vector \mathbf{x} . Equation (2) changes then to

$$\mathbf{x}(t) = \begin{pmatrix} a_1 & 1 \\ a_2 & 0 \end{pmatrix} \mathbf{x}(t-1) + \boldsymbol{\eta}(t), \quad (6)$$

with the vectors

$$\mathbf{x} := \begin{pmatrix} x(t) \\ a_2 x(t-1) \end{pmatrix} \quad \text{and} \quad \boldsymbol{\eta} := \begin{pmatrix} \eta \\ 0 \end{pmatrix}. \quad (7)$$

The Sun is subject to a multitude of solar oscillations. Hence we have to expand the dimension of Eq. (6) further by two dimensions per each excited oscillation mode. If we assume that we have M damped harmonic oscillations excited on the Sun equation (6) then changes to

$$\mathbf{X}(t) = A\mathbf{X}(t-1) + \boldsymbol{\Xi}(t) \quad (8)$$

with

$$\mathbf{X}(t) = \begin{pmatrix} x^{(1)}(t) \\ a_2^{(1)} x^{(1)}(t) \\ x^{(2)}(t) \\ a_2^{(2)} x^{(2)}(t) \\ \cdot \\ \cdot \\ \cdot \\ x^{(M)}(t) \\ a_2^{(M)} x^{(M)}(t) \end{pmatrix}, \quad (9)$$

$$A = \begin{pmatrix} a_1^{(1)} & 1 & 0 & 0 & 0 & \dots & 0 & 0 & 0 \\ a_2^{(2)} & 0 & 0 & 0 & 0 & \dots & 0 & 0 & 0 \\ 0 & 0 & a_1^{(2)} & 1 & 0 & \dots & 0 & 0 & 0 \\ 0 & 0 & a_2^{(2)} & 0 & 0 & \dots & 0 & 0 & 0 \\ \cdot & & & \dots & & & \cdot & & \\ \cdot & & & \dots & & & \cdot & & \\ \cdot & & & \dots & & & \cdot & & \\ 0 & 0 & 0 & 0 & 0 & \dots & 0 & a_1^{(M)} & 1 \\ 0 & 0 & 0 & 0 & 0 & \dots & 0 & a_2^{(M)} & 0 \end{pmatrix},$$

$$\text{and } \boldsymbol{\Xi}(t) = \begin{pmatrix} \eta^{(1)}(t) \\ 0 \\ \eta^{(2)}(t) \\ 0 \\ \cdot \\ \cdot \\ \cdot \\ \eta^{(M)}(t) \\ 0 \end{pmatrix},$$

where the superscript enumerates the single modes.

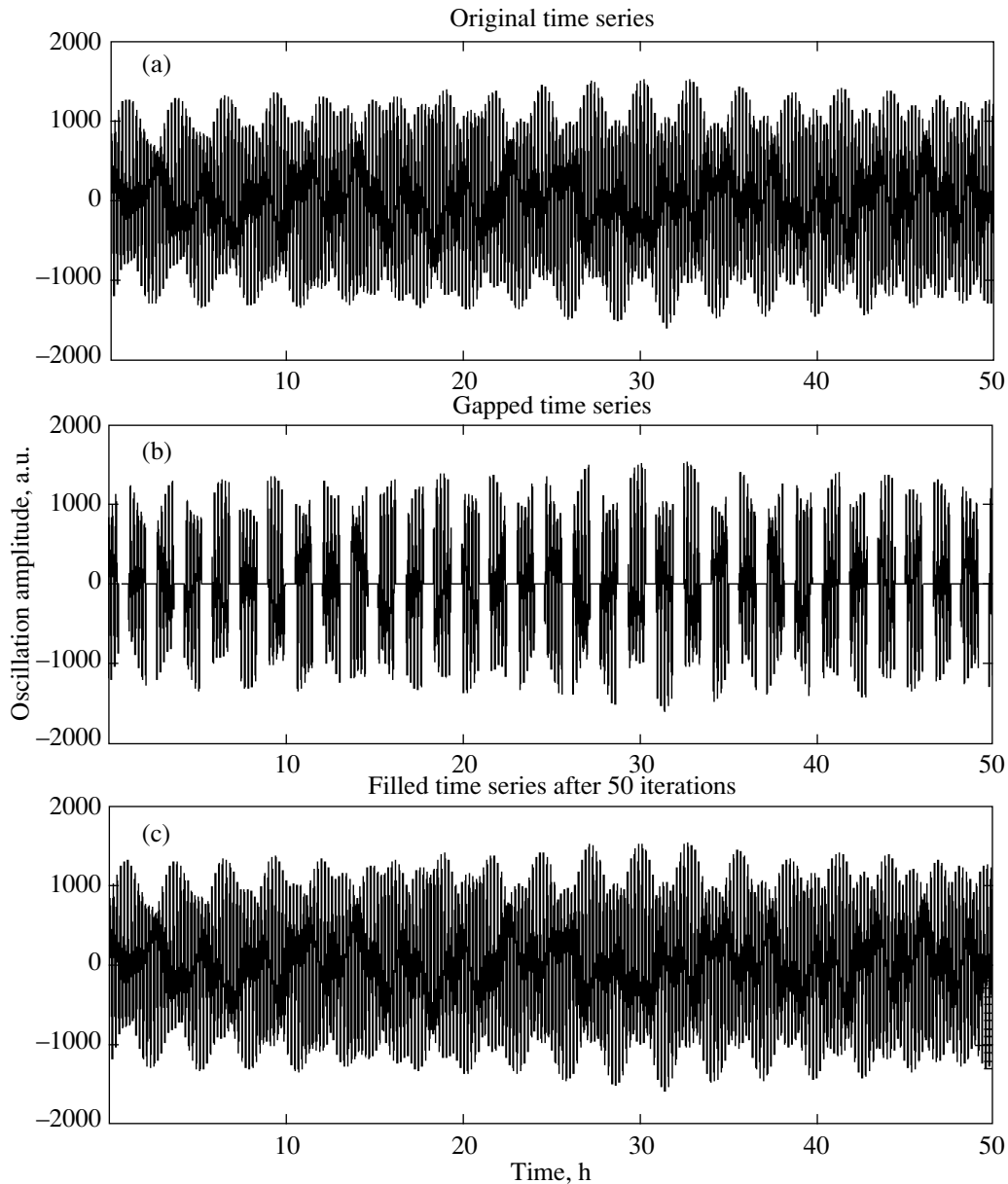


Fig. 1. (a) Artificial oscillation time series $y(t)$ as superposition of the three oscillations $\nu_1 = 1394.7 \mu\text{Hz}$, $\nu_2 = 2693.3 \mu\text{Hz}$, and $\nu_3 = 3984.4 \mu\text{Hz}$. (b) The time series in the top row interrupted every 94 min by artificial gaps of 36 min duration. (c) The recovered time series after 50 iterations of the gap filling algorithm.

The covariance matrix of the components of the noise vector Ξ is defined by $Q := \text{Cov}(\Xi_i \Xi_j)$, where Ξ_i and Ξ_j are components of the noise vector.

Each location on the solar surface oscillates by a superposition of all excited oscillations. Therefore the observation is given by

$$y(t) = C\mathbf{X}(t) + \epsilon(t), \quad (10)$$

where C is a $1 \times M$ array that performs a suitable mapping of the M oscillations to the one-dimensional series $y(t)$; $\epsilon(t)$ is observational noise with $\epsilon(t) \sim N(0, R)$. The Eqs. (6) and (10) form a linear state-

space model (LSSM). We will show in the following section, that given the observation $y(t)$ and an estimate for the matrix C the parameters A , Q , and R of the state space model and the hidden state vector $\mathbf{X}(t)$ and herewith the single oscillations can be estimated with the expectation maximization algorithm.

3. EXPECTATION MAXIMIZATION ALGORITHM

Parameter estimation in AR models has been established by the Burg or the Durbin-Levinson algorithms. Estimation of the parameters in a linear state

Comparison between the input mode parameters, the mean estimated parameters for a gap-free time series, and the mean estimated parameters for a gapped time series.

Input frequency	Estimated frequency	Estimated frequency	Input damping rate	Estimated damping rate	Estimated damping rate
	ungapped time series	gapped time series		ungapped time series	gapped time series
1394.6590	1394.5333 ± 1.8465	1393.9678 ± 2.5231	0.0075	$0.0075 \pm 1 \times 10^{-4}$	$0.0077 \pm 3 \times 10^{-4}$
2693.3100	2693.1779 ± 0.2859	2696.0787 ± 5.1369	0.0395	$0.0395 \pm 3 \times 10^{-4}$	$0.0405 \pm 1.4 \times 10^{-3}$
3984.4030	3984.4192 ± 0.7404	3982.8221 ± 6.7972	0.7216	$0.7216 \pm 1 \times 10^{-4}$	$0.7229 \pm 1.6 \times 10^{-3}$

Note. Frequency and damping rate in μHz . The parameter estimation was repeated 1000 times; gapfilling was stopped after 50 iterations; the lengths of the time series were 50000 data points. Shown are the frequencies (left three columns) and the damping rates (right three columns). Errors are reported as 1σ confidence intervals.

space model is more demanding. One possibility is offered by the expectation maximization (EM) algorithm (Dempster et al., 1977), which is a procedure for estimating parameters for models with hidden variables. The algorithm is based on two iteratively repeated steps. In the E-step the hidden variables are estimated under the assumption that the model parameters are known. In the M-step, the estimates of the hidden variables are taken literally and the model parameters are corrected. This approach was first applied to the LSSM by Shumway and Stoffer (1982): The E-step estimates the expected dynamic variable \mathbf{X} by the Kalman filter on the basis of initial values for the parameters A , Q , C , and R .

For our case of AR processes, the Kalman filter is given via the following equations (Kalman 1960; Honerkamp 1993)

$$\tilde{P}(t) = AP(t-1)A^\dagger + Q, \quad (11)$$

$$K(t) = \tilde{P}(t)C^T[C\tilde{P}(t)C^T + R]^{-1}, \quad (12)$$

$$P(t) = \tilde{P}(t) - K(t)C^T\tilde{P}(t), \quad (13)$$

and

$$\tilde{\mathbf{X}}(t) = A\hat{\mathbf{X}}(t-1), \quad (14)$$

$$\tilde{y}(t) = C\tilde{\mathbf{X}}(t), \quad (15)$$

$$\hat{\mathbf{X}}(t) = \tilde{\mathbf{X}}(t) + K(t)[y(t) - \tilde{y}(t)]. \quad (16)$$

The first three Eqs. (11)–(13) do not contain the data, they only describe the relations between the parameters A , Q , and R for the determination of the Kalman gain K . The Kalman gain weights the error between the actual observation $y(t)$ and the prediction $\tilde{y}(t-1)$ appropriately in order to form an estimate $\hat{\mathbf{X}}(t)$ for the unobserved state vector $\mathbf{X}(t)$. Concluding the E-step, the whole data with length N shall be used for the parameter estimation of the model in order to determine an improved estimate $\hat{\mathbf{X}}(t|N)$ (Harvey, 1989)

$$B = P(t)A^\dagger P(t+1|N)^{-1}, \quad (17)$$

$$\hat{\mathbf{X}}(t|N) = \hat{\mathbf{X}}(t) + B(\tilde{\mathbf{X}}(t+1) - A\hat{\mathbf{X}}(t)), \quad (18)$$

$$P(t|N) = P + B(P(t+1|N) - \tilde{P}(t+1))B^\dagger. \quad (19)$$

In the M-step the parameters A , Q , and R are updated. The iteration ends when a convergence criterion is met. In the end estimates for \hat{A} , \hat{Q} , \hat{R} , and $\hat{\mathbf{X}}(t|N)$ are found. The quality of the model is evaluated by the following criteria: The model should explain all temporal correlations in the data. Therefore, a perfect model results in residuals that obey a white noise distribution. A Kolmogorov-Smirnov test can be used to check, whether the periodogram of the residuals $y - C\hat{\mathbf{X}}(t|N)$ is compatible with a flat white noise spectrum.

4. FILLING GAPS IN DATA

Gaps in data diminish the quality of the estimated model in the following sense: The EM algorithm would converge onto a model that is also capable in explaining the gaps, i.e., the phases of the extracted single modes were such that the superposition of the modes $C\hat{\mathbf{X}}(t|N)$ cancels out in the gaps. However, if enough information about the process is contained in the recorded time series outside the gaps, the original time series of the single modes can be reconstructed iteratively: The goal is it to forecast the process governed by A and ϵ into the gaps and then re-estimating the elements of the matrix A with the EM algorithm. This forecasting is done according to the relation

$$\hat{\mathbf{X}}(t+1|N) = A\hat{\mathbf{X}}(t|N) \quad (20)$$

for all instants in the gaps. Afterwards an estimate \hat{y} for the observation is reconstructed by replacing the recordings at all instants t in the gaps with

$$\hat{y}(t) = C\hat{\mathbf{X}}(t|N) + \hat{\epsilon}(t), \quad (21)$$

where $\hat{\epsilon}(t)$ is an estimate for the observational noise drawn from the distribution $N(0, \hat{R})$. Then, this new

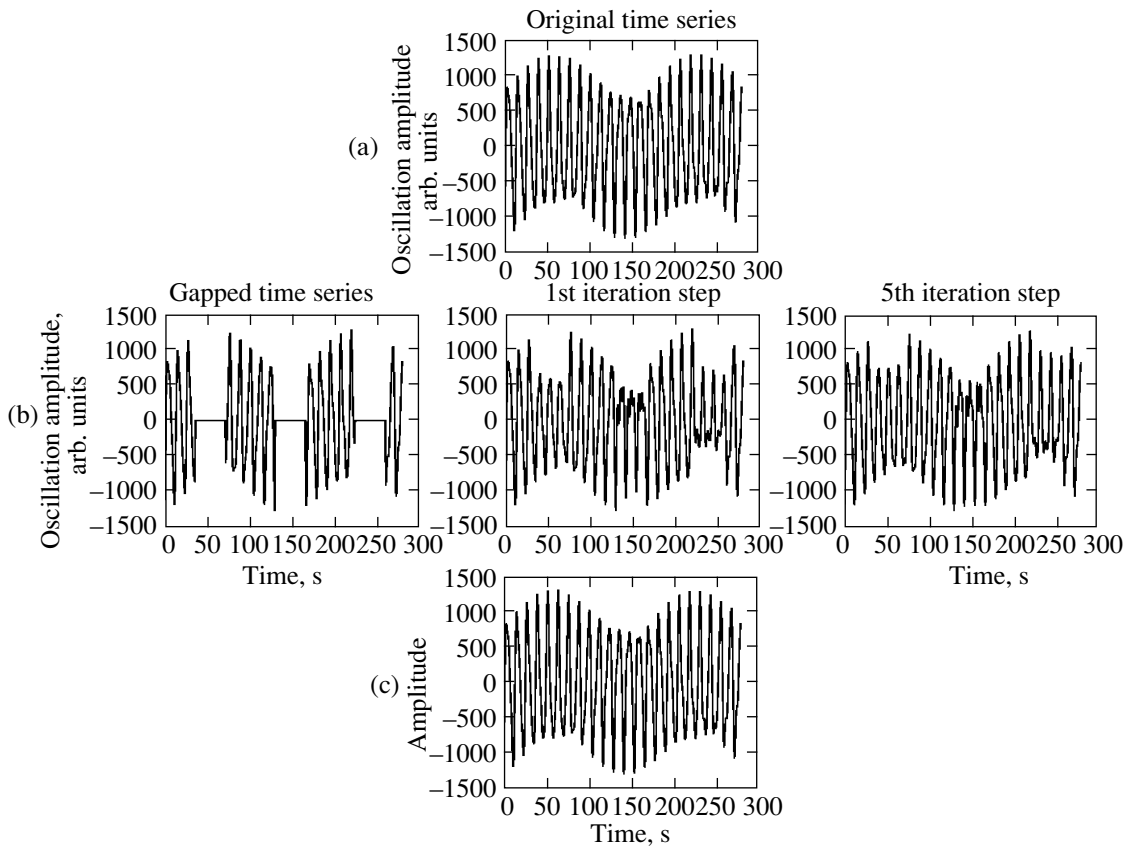


Fig. 2. Top: same artificial time series as in the top of Fig. 1 for the first 280 sec. Middle row: from left to right the gapped time series, and the filled time series for the first and fifth iteration step are displayed. Bottom: the recovered time series after 50 iterations.

observation is used to re-estimate the parameters with the EM algorithm. This shall result in improved estimates as information about the process was filled into the gaps. In the following the steps described in the Eqs. (20)–(21) are repeated.

5. RESULTS

5.1. Numerical Simulations

We demonstrate the power of the gap filling algorithm described above first on the basis of simulated data. We use oscillation frequencies and line widths determined by the BISON network as input for simulating time series with and without gaps. The frequencies and the line widths of each mode are translated into the two AR parameters a_1 and a_2 according to Eqs. (4), (5). Afterwards a time series for each oscillation $x^{(i)}(t)$, ($i = 1, \dots, M$) is generated as realization of Eq. (6) with $Q = \delta_{ij}$ and a sampling rate of 33.5 s. These time series are superimposed and covered with observational noise with $R = 1$ to form an observation time series $y(t)$. Every 94 min the time series $y(t)$ is interrupted by artificial gaps of 64 sampling steps (≈ 36 min) duration, in order to mimic

a time series obtained by a satellite orbiting the Earth. Therefore the duty cycle is $(94 - 36)/94 = 0.62$. Then the procedure to fill these gaps again and to retain the original time series is started with first guesses for the driving noise $Q^{(0)}$, the observational noise $R^{(0)}$, the AR parameters $A^{(0)}$, and the time series $y(t)$ as input.

Figure 1 displays a 50 h long section of a simulated time series $y(t)$ based on the three oscillations with frequencies $\nu_1 = 1394.7 \mu\text{Hz}$, $\nu_2 = 2693.3 \mu\text{Hz}$, and $\nu_3 = 3984.4 \mu\text{Hz}$. The total length of the simulation was 50 000 time steps (≈ 465 h). After 50 iterations the original time series is recovered.

This can be inspected even better in the close-up view in Fig. 2. There, the first three gaps are shown. As displayed in this example, the estimated amplitudes in the gaps are in general too small in the first steps. The explanation for this is the overestimation of the damping rates as long as there are gaps in the time series. Consequently, the prediction fades in the first iteration steps. With better filling of the gaps the estimation of the damping rates improves and the predictions into the gaps become stable.

The gained improvement due to the gap filling algorithm mirrors also in the power spectrum, cf. Fig. 3.

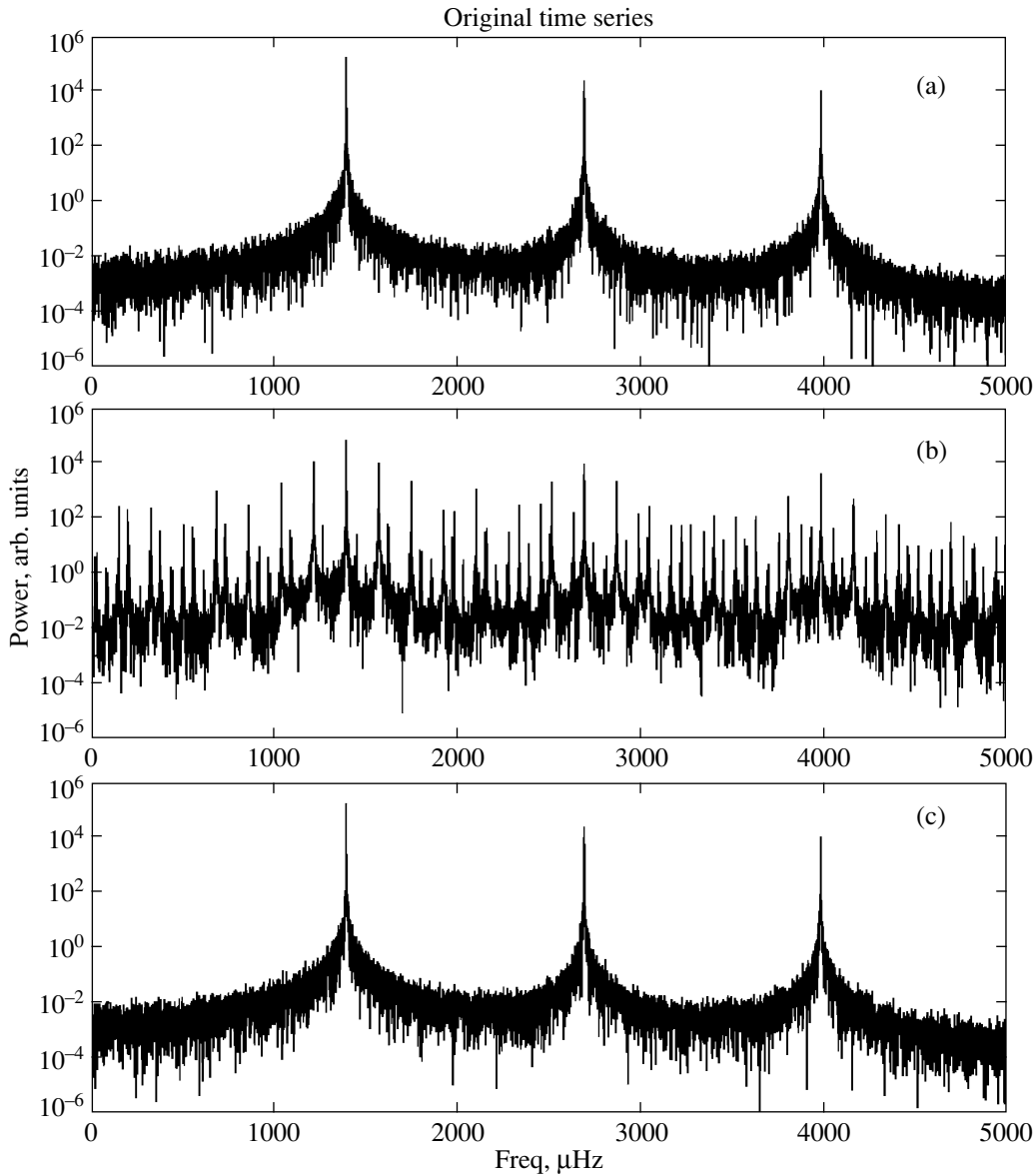


Fig. 3. (a) Power spectrum of the original time series. (b) Power spectrum of the gapped time series. (c) Power spectrum of the recovered time series after 50 iterations.

The gaps affect the power spectrum by introducing multiple side lobes to the major peaks. After filling the gaps the original power spectrum is retained again. Moreover, the reconstruction shows the same noise properties as the original time series.

Besides the time series $y(t)$ the originally unobservable time series for the modes $x^{(i)}(t)$, $i = 1, \dots, M$ can also be recovered. Figure 4 demonstrates how the estimates of a single time series are improved after several iteration steps of the EM algorithm.

In table on page 67 we list the input frequencies and damping rates used for the simulations along

with the afterwards recovered values by the EM algorithm. The parameter estimation by the EM algorithm was repeated 1000 times, hence the average frequencies and damping rates are shown. First, the results are given for recovering the three time series from a simulated observation $y(t)$ without gaps. Second, the results are given for estimating these three oscillations from a simulated observation with gaps introduced (cf. Fig. 5). The EM algorithm was stopped after 50 iterations of gapfilling.

The confidence intervals were determined according to Schlittgen and Streitberg (1987). The original frequencies and damping rates lie within a 1σ interval around the estimated values. Errors are significantly

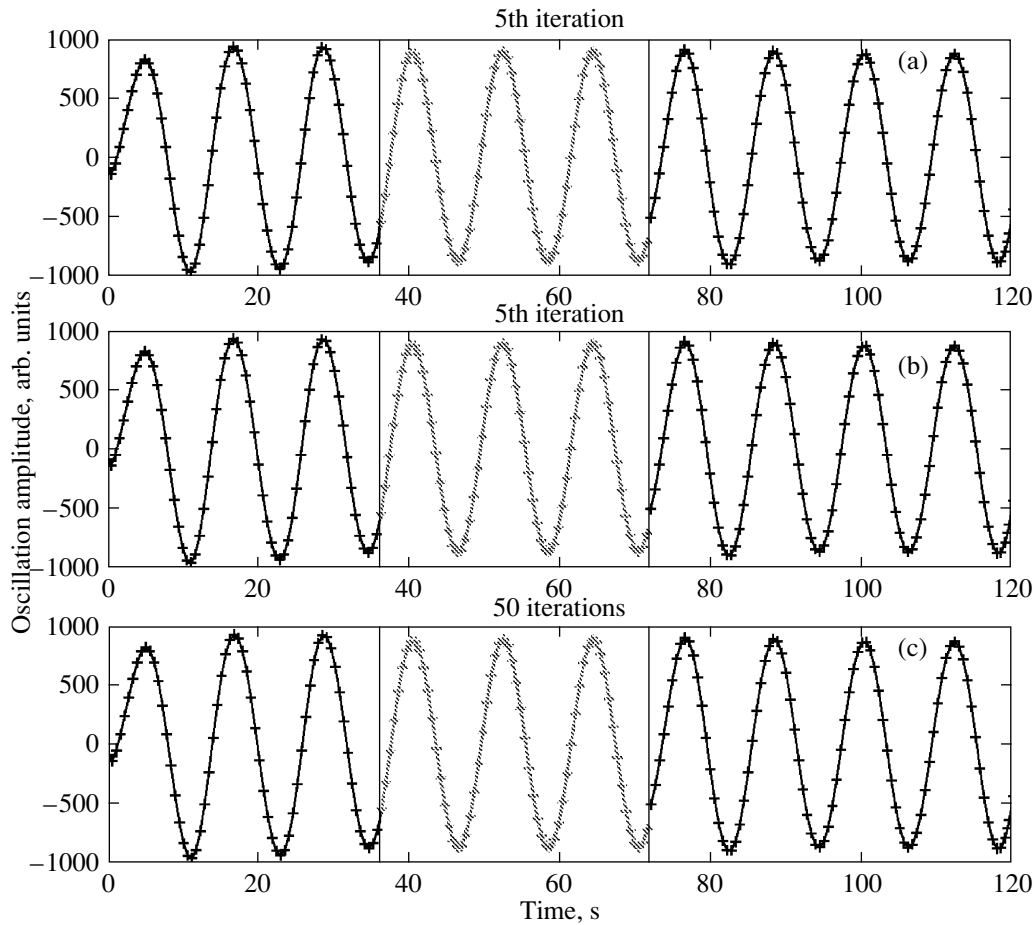


Fig. 4. The first 120 s of the estimated time series of the mode ν_1 after the first (a), fifth (b) and 50th (c) iteration step. The prediction into the gap is marked with gray colors.

higher for the gapped time-series than for the uninterrupted time series, which is explained by the loss of information due to the gaps.

Finally, a Kolomogorov–Smirnov test results in a high probability ($p = 0.9999$) that the residuals $\hat{y}(t) - y(t)$ are drawn from a white noise distribution, i.e., all information on the oscillations available in the observation was extracted to estimate the hidden three time series.

5.2. Filling Gapped Solar Oscillation Data

In our final investigation, we apply the EM algorithm to integrated solar oscillation data. Such time series contain approximately 80 oscillation modes of low harmonic degree. The oscillations were recorded from November 1 until December 12, 2001 as brightness fluctuations in the 350 nm channel of the DIFOS instrument aboard the Russian mission CORONAS-F (Complex Orbital Near-Earth Observations of the Solar Activity) (Lebedev et al. 2004). The sampling rate of the data is 33.5547 s; and as

CORONAS-F is orbiting the Earth, every $T_{\text{orbit}} = 94.607$ min gaps of 36 min duration occur.

A 50 h long section of the original data is illustrated in Fig. 6 along with the time series after filling the gaps with the EM algorithm. The reduced level of the signal in the gaps (cf. Fig. 6) is a result of the final length of the time series, which results in an underestimated mode lifetime. This leads to a too fast decay during the gaps. A longer time series would be necessary to obtain better estimates and to recover the time series as perfect as in the case of the simulations. Nevertheless, estimates for the respective time series of the modes can be extracted. The power spectrum of the original and the filled time series is depicted in Fig. 7. The power at the location of the oscillation modes is increased by approximately a factor of two, whereas the power in the side lobes is partly reduced. The side lobes are not completely removed, as the time series is too short to collect enough information on all the modes. In this case, the frequency can not be determined accurately and the EM algorithm

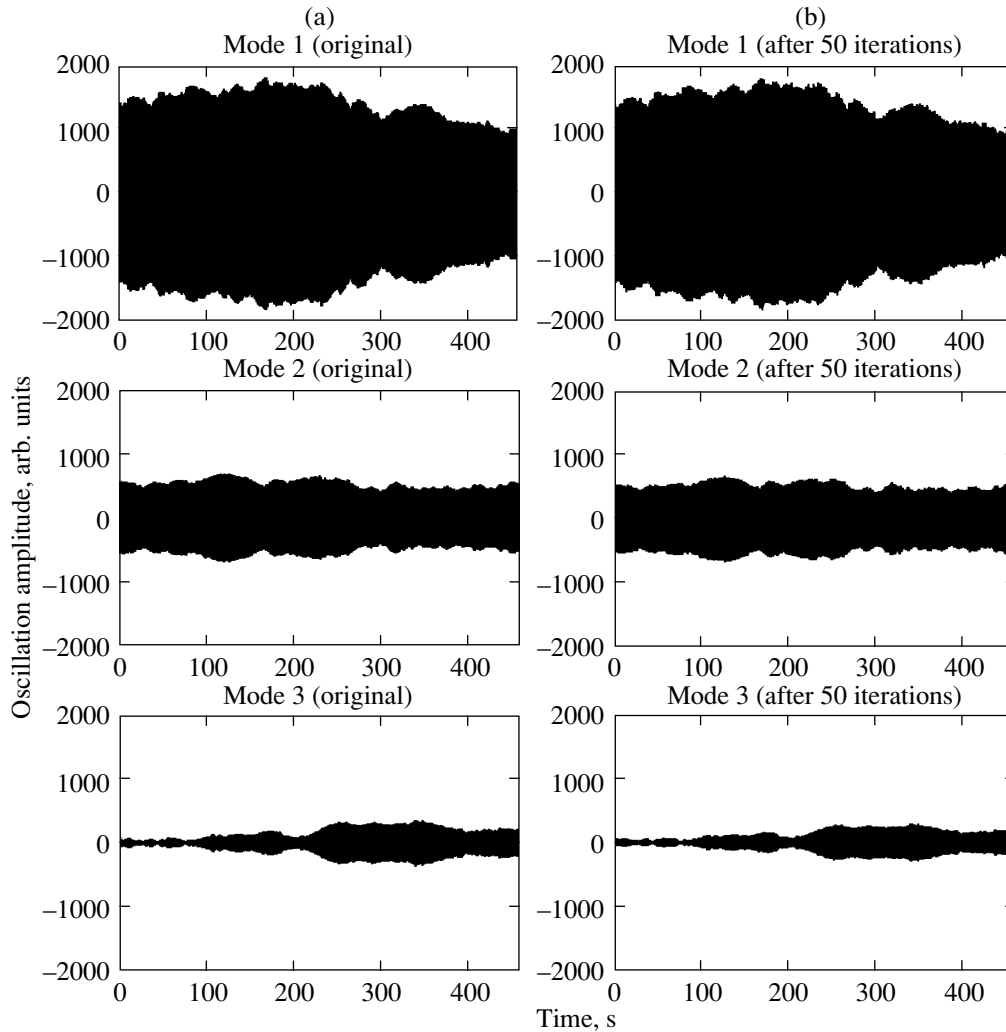


Fig. 5. (a) Original time series. (b) Recovered time series after 50 iterations. The modes from top to bottom are $\nu_1 = 1394.7 \mu\text{Hz}$, $\nu_2 = 2693.3 \mu\text{Hz}$, and $\nu_3 = 3984.4 \mu\text{Hz}$.

might not converge towards the desired solution but rather to a mode with the frequency of a side lobe.

6. DISCUSSION AND CONCLUSIONS

We demonstrated that gaps in solar oscillation data can be filled by predicting the course of the oscillation states into the gaps and by improving these predictions iteratively. The predictions are based on the estimated parameters of the statistical process that describe the solar oscillations. We showed that the gaps can be filled to a perfect match with the original time series, if enough information about the solar oscillations is collected in the whole time series.

The parameter estimation was carried out with the expectation maximization (EM) algorithm. According to the uncertainty principle, the parameter estimation is as better as more information about the oscillations could be collected. Therefore, as longer

the time series as better the estimation of the mode parameters. As gaps reduce the quality of the parameter estimation, the oscillations can not be fully recovered if the time series is too short. Furthermore the length of a gap plays an important role. As the modes are driven by a stochastic noise term, which can not be reconstructed during the gap, the gaps need to be short in comparison to the damping time of the single modes.

One important property of the expectation maximization (EM) algorithm is the possibility to estimate the single oscillation states that are hidden in the observed signal. Therefore, not only the oscillation signal, which is a superposition of all excited eigenmodes of the Sun, can be reconstructed but also the time series and process parameters of the single eigenmodes themselves. As the process parameters estimated by the EM algorithm can be translated into mode frequency and damping rate, the necessary

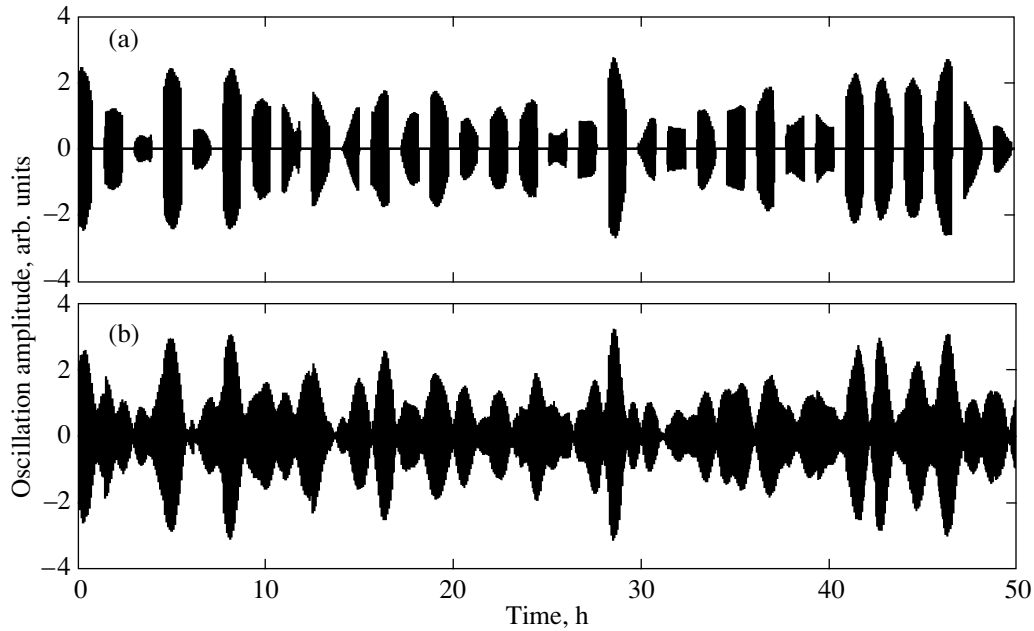


Fig. 6. (a) A section of 50 h duration of the used 42 day DIFOS time series. The gaps are indicated by the horizontal zero level lines. (b) The upper section after filling the gaps with the EM algorithm.

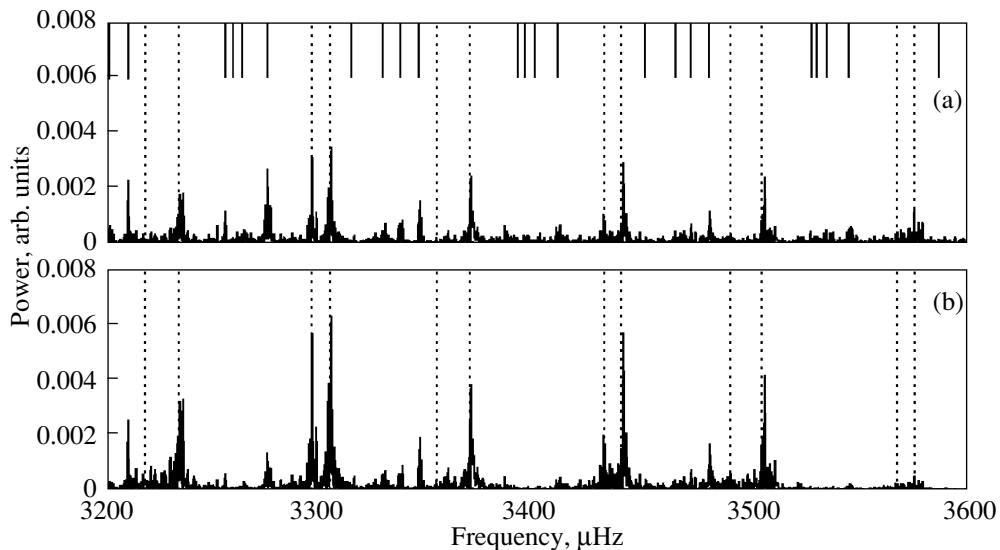


Fig. 7. (a) Power spectrum of the original times series, the locations of the first order side lobes due to the gaps are indicated by the solid bars. (b) Power spectrum of the time series after filling the gaps with the EM algorithm. In both panels the vertical dashed lines indicate the first estimates to the frequencies of the modes used from the BiSON network.

input for helioseismology is therefore derived without using Fourier transformations and fitting the line profile. Furthermore, the estimated covariance matrix Q might allow in future studies of correlations between the modes, e.g., due to common excitation.

We applied the presented gap-filling algorithm to data that simulate recordings from an orbiting satellite observing the Sun in integrated sunlight. Therefore, gaps occur regularly. Nevertheless, the algo-

gorithm can be applied to data with irregularly occurring gaps, too, because the timing of the gaps is irrelevant for the successful convergence of the algorithm. Moreover as presented, the procedure might be interesting for filling gaps of time series from asteroseismology missions, as soon as rough estimates for the eigenfrequencies of the observed stars are available. Furthermore, with more computational effort, resolved oscillation data could also be filled.

ACKNOWLEDGMENTS

M.R. wishes to thank J. Reiter and M. Stix for helpful discussions. The authors thank the anonymous referee for useful suggestions on improving the manuscript. The authors acknowledge support from the European Helio- and Asteroseismology Network (HELAS), which is funded by the European Commission's Sixth Framework Programme. This work was partly supported by RFFI grant nos. 06-02-16359, 09-02-00494.

REFERENCES

1. A. Dempster, N. Laird, and D. Rubin, *J. Roy. Stat. Soc.* **39**, 1 (1977).
2. E. Fossat, S. Kholikov, B. Gelly, F. X. Schmider, D. F. Fraillon, G. Grec, P. Palle, A. Cacciani, S. Ehgamberdiev, J. T. Hoeksema, et al., *Astron. Astrophys.* **343**, 608 (1999).
3. D. F. Fraillon and T. Appourchaux, *Mon. Not. R. Astron. Soc.* **324**, 1159 (2001).
4. M. Gabriel, G. Grec, C. Renaud, A. H. Gabriel, J. M. Robillot, T. Roca Cortes, S. Turck-Chieze, and R. K. Ulrich, *Astron. Astrophys.* **338**, 1109 (1998).
5. A. C. Harvey, *Forecasting Structural Time Series Models and the Kalman Filter* (Cambridge University Press, 1989).
6. J. Honerkamp, *Stochastic Dynamical Systems: Concepts, Numerical Methods, Data Analysis* (John Wiley & Sons, 1993).
7. J. Honerkamp, *Statistical Physics* (Berlin, Springer, 2002).
8. R. E. Kalman, *Trans. ASME J. Basic Eng. Series D* **82**, 35 (1960).
9. N. I. Lebedev, V. D. Kuznetsov, V. N. Oraevski, J. Staude, and R. Kostyk, *Astronomy Reports* **48**, 871 (2004).
10. R. Schlittgen and B. Streitberg, *Zeitreihenanalyse* (R. Oldenburg Verlag, Munchen, 1987).
11. R. Shumway and D. Stoffer, *J., Time Ser. Anal.* **3**, 253 (1982).
12. Y. Zhugzhda, in *ASP Conference Series, GONG'94: Helio- and Astero-Seismology* (1995), Vol. 76, p. 516.